Article:

McAuliffe, L. J., Dolan, J. F., Rhodes, E. J. et al. (3 more authors) (2015) Paleoseismologic evidence for large-magnitude (M-w 7.5-8.0) earthquakes on the Ventura blind thrust fault: Implications for multifault ruptures in the Transverse Ranges of southern California. Geosphere, 11 (5). pp. 1629-1650. ISSN 1553-040X

https://doi.org/10.1130/GES01123.1

Paleoseismologic evidence for large-magnitude (Mw 7.5–8.0) earthquakes on the Ventura blind thrust fault: Implications for multifault ruptures in the Transverse Ranges of southern California

Lee J. McAuliffe[1]
James F. Dolan[1]
Ed Rhodes[2,6]
Judith Hubbard[3,5]
John H. Shaw[3]
Thomas L. Pratt[4]

[1]Department of Earth Sciences, University of Southern California, Los Angeles, CA 90089

[2]Department of Earth, Planetary and Space Sciences, University of California Los Angeles, Los Angeles, CA 90095

[3]Department of Earth & Planetary Sciences, Harvard University, Cambridge, MA 02138

[4]U.S. Geological Survey, Reston, VA

[5]Earth Observatory of Singapore, Nanyang Technical University, Singapore

[6]Department of Geography, University of Sheffield, Sheffield, S10 2TN, UK

Keywords: Paleoseismology, neotectonics, western Transverse Ranges, Ventura fault, San Cayetano fault, blind thrust fault

Abstract

Detailed analysis of high-resolution seismic reflection data, continuously cored boreholes and cone penetrometer tests (CPTs), and luminescence and ^{14}C dates from Holocene strata folded above the tip of the Ventura blind thrust fault constrain the ages and displacements in the two most recent earthquakes. These two earthquakes are recorded by a prominent surface fold scarp and a stratigraphic sequence that thickens across an older buried fold scarp, and occurred soon after about 700-900 years ago (most recent event) and between 3-5 ka (penultimate event). Minimum uplift in these two scarp-forming events was ~6 m for the most recent earthquake and ~4.5 meters for the penultimate event. Individual uplifts of this amount require large magnitude

earthquakes, probably in excess of M_w7.5 and likely involving rupture of the Ventura fault together with other Transverse Ranges faults to the east and west. The proximity of this large reverse-fault system to major population centers, including the greater Los Angeles region, and the potential for tsunami generation during ruptures extending offshore along the western parts of the system, highlight the importance of understanding the complex behavior of these faults for probabilistic seismic hazard assessment.

1 Introduction

1.1 Recognition of emerging thrust fault hazards

The recognition of the hazards posed by thrust fault earthquakes to urban centers around the world has been highlighted by several recent events (e.g., 1994 M_w 6.7 Northridge, 1999 M_w 7.6 Chi-Chi, 2005 M_w 7.5 Kashmir, 2008 M_w 7.9 Wenchuan). These earthquakes demonstrate the need to better understand the behavior of these faults and their associated folds, particularly when these faults are "blind", that is, the faults do not reach (or "see") the surface. The 2008 M_w 7.9 Wenchuan earthquake further illustrated that thrust fault ruptures may link together adjacent faults to generate extremely large-magnitude earthquakes. In southern California, the prospects for large, multiple-segment thrust fault ruptures remain poorly understood. The numerous large reverse and oblique-slip faults in the Transverse Ranges suggest that such large earthquakes are possible, and would represent a serious hazard to property and life in the densely populated southern California region.

Most seismic hazard assessments and models of reverse fault earthquakes in southern California involve the rupture of individual faults in the Transverse Ranges in moderately large magnitude ($\geq M_w$ 7) events (e.g., Sierra Madre fault, San Cayetano fault; WGCEP, 1995).

Although the seismic threat posed by these individual faults is significant, as was demonstrated by the 1994 M_w6.7 Northridge earthquake, which was the costliest natural disaster in US history prior to Hurricane Katrina [Scientists of the U.S. Geological Survey and the Southern California Earthquake Center, 1994], a larger threat presents itself if several of these faults rupture together. The reverse and oblique-slip faults of the Transverse Ranges form an interconnected, >200-km-long network of faults that could potentially rupture together to cause large-magnitude events. While the potential for these faults to link and rupture together has recently been recognized (e.g., Dolan et al., 1995; Hubbard et al., 2014), relatively little is known about the ages, repeat times, and magnitudes of paleo-earthquakes generated by faults within the Transverse Ranges.

In this paper, we apply a multi-disciplinary approach utilizing continuously cored borehole and cone penetrometer test (CPT) data, in conjunction with high-resolution and deeper-penetration petroleum industry seismic reflection data, to document the structural evolution of young folds formed by the Ventura fault, a major reverse fault in the western Transverse Ranges. Together, these new data allow us to assess the geometry of buried fold scarps and identify periods of stratigraphic growth that record discrete uplift events along the Ventura fault. We use these data to determine the timing and displacements of Ventura fault paleo-earthquakes and discuss these results in light of their implications for assessing the prospects for multi-segment ruptures in the western Transverse Ranges, and more generally for seismic hazard in southern California.

1.2 Regional Geology

The western Transverse Ranges are dominated by several major east-west faults and folds that extend “transverse” to the general northwesterly structural grain of coastal California. These structures are evidence of the north-south compressive forces that have been responsible for the observed deformation since early Pliocene time (Luyendyk et al., 1985). The deformation of Pleistocene and younger deposits along a similar structural grain, together with current geodetic data, illustrate the ongoing style of deformation within this region.

Located about 75 km northwest of Los Angeles, the Ventura basin is a narrow, ~50-km-long basin bounded on both the north and south by a complex network of E-W reverse and oblique-left-lateral reverse faults (Figure 1). These structures include the Oak Ridge to the south, and the faults responsible for uplift of the Ventura Avenue Anticline (VAA) and Topa Topa mountains to the north. The Ventura basin is ~4 km across at its widest near the city of Ventura, and narrows towards its eastern end where the northern basin-bounding San Cayetano fault overrides the south-dipping Oak Ridge fault (Huftile and Yeats, 1995).

The Ventura basin, which is >10 km thick at its deepest point, is thought to have formed during the mid-Miocene clockwise rotation of the western Transverse Ranges block to its current east-west trend and experienced oblique, north-south shortening since the Pliocene (Hornafius et al., 1986; Jackson and Molnar, 1990; Luyendyk, 1991). Geodetically determined north-south convergence across the Ventura basin is as high as 7 to 10mm/yr (Donnellan et al., 1993a; 1993b; Hager et al., 1999; Marshall et al., 2008). The Ventura Avenue Anticline, located on the north side of the basin (Figure 1), is rising at a rapid rate of ~5 mm/yr. This structure, which is underlain by the Ventura fault, is thought to accommodate much of the north-south shortening across the western basin (Rockwell et al., 1988; Stein and Yeats, 1989; Hubbard et al., 2014).

The blind Ventura fault is a ~12 km long, east-west-striking, north-dipping reverse fault that is expressed at the surface by a monoclinal fold scarp extending across the city of Ventura (Ogle and Hacker, 1969; Sarna-Wojcicki et al., 1976; Yeats, 1982; Perry and Bryant, 2002). Some studies suggested that the Ventura fault is a shallow fault rooted in the syncline at the southern end of the Ventura Avenue Anticline (e.g., Yeats, 1982; Huftile and Yeats, 1995), and thus does not pose a major earthquake threat. Others, however, have suggested that is it a seismogenic structure in its own right (Sarna-Wojcicki et al., 1976; Sarna-Wojcicki and Yerkes, 1982). Historically, several different models have been proposed for the geometry of the Ventura fault at depth (e.g., Yeats, 1982; Huftile and Yeats, 1995; Sarna-Wojcicki and Yerkes, 1982). Hubbard et al. (2014), combined constraints from these previous models along with new seismic and well data to interpret the Ventura fault as a major seismic source that extends to the base of the seismogenic zone as a single planar surface dipping 50°±5° N.

We interpret the Ventura fault to be the dominant structure accommodating shortening and uplift of the VAA by fault-propagation folding based on a comprehensive set of geologic maps, industry well and seismic reflection data, and high-resolution seismic reflection profiles described in Hubbard et al. (2014). Terrace uplift rates show a decrease in the uplift rate of the anticline at ~30 ka (Rockwell et al., 1988), which is consistent with a breakthrough of the Ventura fault to the near surface at that time (Hubbard et al., 2014). This breakthrough shifted the tipline of the Ventura fault to the south, corresponding to the monoclinal fold scarp in the city of Ventura. The fault remains buried by a thin sedimentary cover, however, and is therefore blind.

Regionally, the Ventura fault acts as a transfer structure to accommodate significant north-south shortening as slip is transferred between the San Cayetano fault to the east and Pitas Point and related faults to the west. Hubbard et al. (2014) suggested that these faults all merge below 7.5 km depth onto a regional detachment to form a nearly continuous fault surface despite having separate surface traces. Previous slip rates on the Ventura fault have been calculated at 0.2-2.4 mm/yr (Peterson and Wesnousky, 1994; Perry and Bryant, 2002). Hubbard et al. (2014), in contrast, determined a fault slip rate of ~4.1-8.1 mm/yr for the past 30±10 ka based on the terrace uplift rates and our updated interpretation of the fault kinematics.

2 Results

2.1 Day Road study area

The City of Ventura extends east-west along the base of the steep, south-facing mountain front at the western end of the Ventura basin. This mountain front is coincident with the forelimb of the VAA. The city itself is built mainly on low-relief, latest Pleistocene to Holocene alluvial fans deposited from over half a dozen rivers and creeks draining southward from the VAA. Most of these alluvial fans exhibit drainages that have been incised by ~one to six meters into remnant fan surfaces, with the exception of the source drainage for the alluvial fan emanating from the north end of Day Road (Figure 5 and Supplementary figure S1). We refer to this latter fan as the Arroyo Verde Fan after the city park located within the source drainage.

The topographic expression of the Ventura fault through the city is marked by a prominent south-facing scarp that extends roughly eastward for ~12 km from the eastern edge of the active channel of the Ventura River to where the mountain front takes ~2 km step to the north at the eastern end of the City of Ventura (Figure 1). At the eastern end of the scarp it appears that slip is transferred northwards in left-stepping, en echelon fashion onto the Southern San Cayetano fault. This latter fault is interpreted as a major north-dipping blind thrust, perhaps with a south-dipping backthrust in the uppermost few kilometers that serves to transfer slip between the Ventura-Pitas Point fault to the west and the rapidly slipping eastern San Cayetano fault to the east (Hubbard et al., 2014).

After collecting high-resolution seismic reflection profiles at three sites along the Ventura fault scarp (McAuliffe, 2014), we chose Day Road as the preferred site for our borehole and CPT study due to its location on an active alluvial fan with the potential for continuous deposition; elsewhere along the fault, south-flowing drainages have incised into the alluvial fan surfaces, isolating them from active deposition (Figure 5 and Supplementary figure S1). The absence of incision into the Arroyo Verde Fan suggests that the surface was deposited more recently than those fans that are incised. This young fan deposition presents an ideal target for resolving the most recent slip history of the Ventura fault.

2.2 High resolution seismic reflection

We collected a 2.24 km-long, high-resolution seismic reflection profile along Day Road as part of a broader effort to characterize the deformation of strata above the tipline of the Ventura fault. However, the data quality at Day Road was poor because of high traffic noise and signal attenuation within the unsaturated alluvial fan strata. In contrast, our high-resolution profile collected along Brookshire Avenue, 1.4 km east of our Day Road site, yielded a better quality image of the structure beneath the scarp (Figure 5). The Brookshire Avenue profile extends northward along Brookshire Avenue for 1.06 km from its intersection with Woodland Street, to the north end of Brookshire Avenue where it intersects Kearny Street (Figures 2 and 3a). Due to the linearity of this transect and the low traffic noise on this quiet street, this profile produced a better image than the nearby Day Road profile.

At Brookshire Avenue our high-resolution seismic profiles reveal a panel of south-dipping beds between two panels of sub-horizontal strata. This profile provides a clear image to a depth of ~500 m. A well-defined, north-dipping active synclinal axial surface can be traced from the tipline of the fault at a depth of approximately 230 meters below sea level to the surface

(Figure 5). The south-dipping strata between the synclinal and anticlinal axial surfaces extends to the surface at the prominent south-facing fold scarp, which at this location occurs approximately 500 meters south of the topographic range front. This scarp defines the surface expression of deformation associated with the most recent folding events on the underlying thrust ramp.

Using the structure visible on the Brookshire profile as a guide to the overall structure, a similar structure can be interpreted on the poorer quality Day Road profile. The latter profile shows weak south-dipping reflectors on the northern part of the profile and flat strata on the south. The boundary between these dip domains defines an axial surface that reaches the ground surface around distance mark 2600 m.

2.3 Borehole excavations

To determine the geometry of recent folding of Arroyo Verde fan strata above the Ventura fault tipline at Day Road, we acquired six, 8-cm diameter, 15- to 21-m-deep, continuously cored hollow-stem auger boreholes along the central section of the Day Road transect across the prominent fold scarp (Figures 3 and 4). The cores facilitated detailed observation of the subsurface structure and stratigraphy through correlations of the upper 20 meters of alluvial strata. In addition to allowing sampling for radiocarbon and luminescence dating, the continuous sampling method allowed us to observe basic sediment characteristics, including grain size, sediment color, and degree of soil development. These sediment characteristics were used to identify and correlate the subsurface stratigraphy between the six boreholes.

We also conducted 13 Cone Penetration Tests (CPTs), which provided detailed measurements of grain size variations and other sediment characteristics with depth. The much-denser spacing of the CPTs provided valuable data that allowed much more robust correlations of strata between boreholes. In addition, we excavated two, 1.8-m-deep, 1 m x 1 m sampling pits at the top and base of the surface fold scarp to determine whether any post-MRE erosion or deposition has taken place. At each pit we collected sediment samples for luminescence dating, and logged the upper 1.8 m of sediment.

2.4 Stratigraphic observations

The borehole-CPT transect at Day Road extends a total of 368 meters from the northernmost borehole at 34.281901° N, 119.227480° E, which is located ~210 m north of the top of the fold scarp, to the southernmost borehole at 34.278844° N, 119.227021° E about 150 m south of the base of the fold scarp (Figure 3a and 4). The fold scarp at the Day Road site lies at the north side of the intersection of Day and Loma Vista Roads, with Loma Vista Road extending approximately along the base of the scarp.

The stratigraphy along Day Road consists of alternating silt and fine- to coarse-grained sand beds interbedded with several granule-pebble gravel layers. The results from our borehole and CPT analyses can be generalized to show that nine distinctive stratigraphic packages can be traced along the entire length of the transect. The uppermost 4 m of section consist predominantly of fine-grained sands and silts (Units A and B). These are underlain by a sequence of sandy- to coarse-grained gravelly units (Units C, D and E), which in turn overlie a prominent fine-grained silty interval (Unit G).

The sedimentary section is thicker on the downthrown side of the scarp, and there the package comprising Units C and D is separated into three distinct layers referred to as D1, D2 and D3. These three sub-units appear to fan downslope and may represent onlapping of material onto a paleo-event scarp, as discussed below. The correlations were aided by gypsum in the upper 0.5 m of Unit C between boreholes DY-2B and DY-3, and by distinctive 0.5- to 3-cmsized detrital chips of what appear to be fire-baked clay from the mountains north of Ventura found between 6 and 10 m depth in boreholes DY-2, DY-2B, DY-2C and DY-3 (letter B in Figure 7). Unit G is a distinctive fine-grained, predominantly silt interval that was deposited on top of a sand- to pebble-gravel unit (Unit H), which in turn overlies fine-grained silt Unit I.

3 Age Control

Age control for the Day Road transect is provided by 18 Infra-Red Stimulated Luminescence (IRSL) samples and eight radiocarbon ages from small detrital charcoal fragments collected from the six boreholes and the two sampling pits (Table 1). The recently developed post-IR $IRSL_{225}$ dating approach for potassium feldspar (Buylaert et al., 2009; 2012; Thiel et al., 2011), modified for single grain application, was used to date our luminescence samples (Rhodes, submitted; Brown et al., submitted).

3.1 IRSL dating of sediment

IRSL samples were removed from 15cm steel or brass core tubes under low-intensity amber laboratory lighting, and sieved to isolate the 175-200µm grains. After initial HCl treatment, the fraction <2.58 g.cm^{-3} was isolated for each sample using lithium metatungstate (LMT) solution, and treated with 10% hydrofluoric acid (HF) for 10 minutes to remove the outer alpha-irradiated layer. Following rinsing, drying and second sieving, grains >175µm were mounted in Risø single grain holders.

Measurements were performed in a Risø TL-DA-20CD automated reader equipped with an XY single grain attachment. Stimulation used a 150 mW 830 nm IR laser directed through a RG780 filter. After an initial preheat at 250°C for 60 seconds, each grain was stimulated with IR light for 2.5s at 50°C to remove charge most susceptible to fading by localized tunneling (Jain and Ankjærgaard, 2011). Following the first IR stimulation, each grain was again stimulated at 225°C for 2.5s to release the electrons from more stable traps (Buylaert et al., 2009; 2012; Thiel et al., 2011). Luminescence emissions were observed using an EMI 9235QB photomultiplier (PMT) fitted with a BG3 and BG39 filter combination allowing transmission between 340 and 470nm. The dating protocol used a single aliquot regenerative-dose (SAR) approach, incorporating full sensitivity correction measurements using a test dose, a final hot bleach within each SAR cycle using Vishay TSFF 5210 870nm IR diodes for 40s at 290°C, with multiple regenerative dose steps, a zero dose to assess thermal transfer, and a repeat of the first artificial dose point.

Samples displayed consistent behavior, with many grains providing intense IRSL decays at both 50 and 225°C, displaying exponential-plus-linear signal growth with dose. Between 200 and 600 grains were measured for each sample. A significant subset of single grain equivalent dose (D_e) values for each sample was consistent with each other around the minimum D_e, and this value, determined assuming an overdispersion value 15%, was used in age estimation. Fading assessment was made of each grain using delay times of several days, though very little laboratory fading was observed, and fading was assumed to be absent for the post-IR IRSL signal from these samples. IRSL results are consistent with a radiocarbon age from a charcoal sample collected at 13.51 m depth in borehole DY-4. Specifically, this charcoal sample (DY-C7) yielded a calibrated calendric age of 6899-7158 Cal. Yr. BP. This sample, which comes from the basal part of Unit G, is ~1,000 years younger than a 7930 ± 530 IRSL age (DY-OSL-1/5) from the top of underlying Unit H, and is ~2,000 years older than overlying IRSL samples from near the top of Unit G (4790 ± 350 [DY-OSL-4/3] and 5020 ± 310 [DY-OSL-1/4]).

The luminescence ages revealed that the borehole transect spans almost the entire Holocene, with the youngest samples collected from the middle of Unit A in the sample pits at a depth of 1.1 m having ages of 770 ± 90 and 790±170 years, and the oldest sample from a depth of 18.21 m in borehole DY-1 yielding an age of 11,720 ± 770 years before 2013 (yb2013).

3.2 Radiocarbon ages

Only eight of the 28 radiocarbon samples that were sent to the Keck Carbon Cycle AMS facility at the University of California, Irvine, yielded allowable ages (Table 1). The remaining samples did not provide suitable ages because either the samples were too small and/or no organic material was left after the standard acid-base-acid pre-treatment. Several of those samples that did provide ages have extremely large uncertainties due to the small sample size (e.g., DY-C12 and DY-2C:CL-1). Furthermore, many of the radiocarbon samples appear to have been reworked because they show ages that are much older than other radiocarbon ages and luminescence dates from shallower strata. For example, the 44128-48526 BP age of sample DY-C14, the >54702 BP age of sample DY-2C:CL-01, and the >52792 BP age of sample DY-C12, are all much older than the mid- to late-Holocene strata within which they were found. In addition, the 8051-8409 BP age of charcoal sample DY-C1 is >1000 years older than underlying charcoal sample DY-C7, which yielded an age of 6899-7158 Cal. Yr. BP. Finally, the 1335-1415 BP radiocarbon age for sample DR-14:CL-01 from the northern pit is several hundred years older than the internally consistent c. 1000-year-old IRSL ages from samples of the underlying silt bed (pit samples DR13-04 and DR14-04). All the radiocarbon results in Table 1 have been corrected for isotopic fractionation according to the conventions of Stuiver and Polach (1977), with $\delta^{13}C$ values measured on prepared graphite using the AMS.

3.3 Chronological synthesis

These age data reveal that the uppermost part of the Arroyo Verde alluvial fan is Holocene in age and that the fan has been actively receiving sediment within the past c. 800 years. The luminescence and radiocarbon ages provide evidence for relatively steady sediment accumulation rates throughout the Holocene.

The absence of any well-developed soils within the upper 20 m suggests a rapid rate of sediment accumulation, without any substantial hiatuses. In coastal environments along the Ventura basin, soil development occurs at much faster rates relative to soils of equivalent age in California's inland areas (Rockwell et al., 1985). Favorable soil development conditions are promoted by the presence of sodium ions (a clay deflocculant) caused by sea fog in these coastal areas (Rockwell, 1983). There is little evidence for the development of significant soils within the generally pale-colored sediments at the Day Road site despite the coastal setting, suggesting that sediment accumulation during alluvial fan aggradation has been relatively continuous and rapid. Rapid sediment accumulation is also consistent with our geochronologic results showing a relatively young section. Although we cannot rule out potential minor stripping of paleosols in this alluvial environment, the absence of any significant soil development is consistent with the relatively continuous sediment accumulation during the Holocene shown by our luminescence and ^{14}C data.

The four IRSL ages from the two sample pits warrant additional discussion. In each pit, we dated two samples, one from ~1.1 m depth in a silt bed, and a second from ~1.6-1.8 m depth in a different silt layer beneath a weakly developed soil. Despite the 275 m distance between the sample pits, the resulting pairs of ages are remarkably consistent, with the two shallow samples yielding ages of 790±170 and 770±90 years before AD 2013 (DR14-02 and DR13—02, respectively), and the lower samples in each pit yielding ages of 1030±90 years before 2013 (DY14-04) and 1020±120 years before AD 2013 (DY13-04). This internal consistency, and the similar stratigraphy of the two pits, strongly suggests that these are the same strata, encountered at the same depths, both above and below the scarp. The absence of thickening of this latest Holocene section on the downthrown side of the scarp indicates that these strata were deposited before the scarp developed in the most recent earthquake. The deepest identifiable sedimentary unit that can be correlated along the entire transect is Unit I, which is dated at ~9ka.

4 Interpretation

4.1 Most recent event (Event 1)

Several observations from the two shallowest units in our cross-section show evidence for folding of sediments during the most recent event on the Ventura fault at Day Road. Specifically, the stratigraphy of the uppermost 4 m (Units A and B in Figure 7) tracks the ground surface across the fold scarp without a significant change in thickness indicating that: (1) these strata were deposited on the gently south-dipping slope of the Day Road alluvial fan and were subsequently folded; (2) the fold scarp has not yet been buried by young Day Road alluvial strata following the most recent event(s); and (3) the ~6.0-6.5 m height of the fold scarp (measured vertically from the northward and southward projections of the average far-field ground surface slope) records the amount of uplift during the most recent large-magnitude earthquake (or earthquakes) on the Ventura fault. The remarkably consistent pairs of IRSL ages from the uppermost 1.1 to 1.8 m collected from the sample pits above and below the scarp suggest minimal post-MRE erosion of the hangingwall and negligible post-MRE deposition on the footwall after the scarp formed. The absence of thickening in these latest Holocene strata supports our interpretation that deposition of these beds pre-dates the scarp, and thus that the height of the current topographic scarp records the approximate amount of uplift during the most recent event on the Ventura fault. Moreover, the internally consistent ages from the youngest folded strata in the sample pits ages indicate that the MRE occurred soon after deposition of these beds c. 800±100 years ago (Table 1). We cannot determine whether this large uplift occurred in a single earthquake, or more than one event, because of the absence of growth strata across the scarp. If the fold scarp developed in two events, then both must have occurred in the past ~800±100 years.

4.2 Event 2

Evidence for an older event (or events) at Day Road comes from a second episode of uplift and folding that is recorded by stratigraphic growth of Unit C, which thickens by ~4.5 m southward across the fold scarp (Figure 7). We interpret this sedimentary growth as evidence for deposition against a now-buried paleo-fold scarp that developed during the penultimate folding event(s). The event horizon for this period of fold growth is located in the lower part of Unit C at the base of the growth interval at ~ 8.2 m depth in borehole DY-4. The event horizon is above Unit D3, which is folded parallel to underlying strata at the scarp and has been truncated on the upthrown side by erosion of the hangingwall (Figure 7). Thickening of Unit C by ~4.5 m on the downthrown side of the scarp indicates that at least this much uplift occurred during fold growth. This is a minimum estimate because we cannot quantify the amount of erosion of Unit C that may have occurred on the upthrown side of the fold scarp. Up to 1.3 m of erosion is indicated by the buttressing of Unit D2 (suggesting that it had to be deposited onlapping the paleo-scarp) and the consistent thickness of Units D3 and the lowest parts of Unit C (suggesting that these strata were deposited at the gently sloping pre-earthquake gradient).

Below the growth section in Units D and C, the underlying ~ 7-m-thick sequence of strata in Units E, G, H and I does not change thickness across the fold, indicating that those units were deposited during a period of structural quiescence.

4.3 Possible 3rd Event

Several lines of evidence suggest the possibility of a third event during deposition of the growth interval comprising Units C and D described above. Specifically, stratigraphic correlations show a distinct change in bed dip between Units D2 and D3 within the growth stratigraphic section (7.62 m to 9.75 m in DY-3). This change in bed dip may be due to an additional event and the process of limb rotation (Novoa et al., 2000) just prior to the deposition of Unit D2, causing the beds beneath the event horizon at 7.62 m to 9.75 m in DY-3 depth to have distinctly steeper dips than those above. Alternatively, fanning of material off the paleo-fold scarp may have produced the change in bed dip. These growth strata geometries are not definitive, however, and folding and subsequent deposition of the growth section could all be due to a single earthquake on the Ventura fault (i.e., Event 2).

4.4 Uplift measurements and fault displacement estimates

We determine the total minimum scarp height for each paleo-folding event by projecting the far-field alluvial fan surface slope above and below the scarp and measuring the vertical difference between these two lines as shown on figure 6. For the MRE, the present-day topographic scarp developed some time after deposition of Unit A. Very little, if any, sedimentary growth has occurred since the deposition of this shallowest unit, as shown by both the similar ages of samples collected at ~1.1 m depth from our sample pits above and below the scarp and the overall geometry of the strata relative to the surface scarp (Figure 6 and Table 1).

We therefore use the top of Unit A at the current ground surface as the restoration horizon for the MRE.

Measuring uplift in the penultimate event is slightly more complicated due the apparent truncation of Unit D on the upthrown side of the scarp. With material having been eroded off the hangingwall, any uplift measurements recorded by the remaining Unit C and D strata will be minima. Based on sedimentary growth occurring from the top of Unit D3 to the base of Unit B, we measure the minimum uplift in the penultimate event as ~4.5 m.

To convert the scarp heights to reverse displacements on the underlying Ventura fault, we divide the scarp height by the cosine of the 50°±5° dip of the fault from Hubbard et al. (2014). We also make the conservative assumption that coseismic slip is constant on the fault ramp, rather than increasing with depth as is observed for the total slip accumulated over geologic time scales (Hubbard et al., 2014). This will render any displacement measurements we make minima. For the MRE, 6 m of uplift yields a fault displacement of 7.3-8.5 m (the range in displacement is due to the uncertainty in fault dip angle). For the penultimate event(s), the minimum 4.5 m of uplift yields 5.5-6.4 m of thrust slip (Table 2), although we reiterate that this is a minimum because it does not account for possible erosion of the hangingwall. For example, increasing the height of the paleo-fold scarp by 1 m would result in an estimate of total thrust displacement in the penultimate event that is ~20% larger.

4.5 Paleo-magnitude estimates

We can estimate paleo-magnitudes for the two most recent events on the eastern part of the Ventura fault at Day Road by using published empirical equations based on global regressions that relate earthquake magnitude, fault area, and average displacement (Wells and Coppersmith, 1994; Biasi and Weldon, 2006). Although the calculated displacements at the Day

Road site are only single measurements along the 60-km-long fault Ventura-Pitas Point fault system, which likely exhibits some degree of lateral variability in displacements, even larger uplift values for the four most-recent earthquakes at Pitas Point (Rockwell et al., 2011) suggest that the slip values of 7.3-8.5 m derived from our uplift measurements are suitable for use as the average slip during a system-wide rupture of the Ventura-Pitas Point fault. These values are within the “most likely” range suggested by Hubbard et al. (2014) of 6.2-9.9 m based on uplifted coastal terraces.

Results from two different empirical equations relating earthquake magnitude and average displacement are shown in Table 2. Using the simplifying assumption that the entire Ventura fault slipped with an average displacement of 7.3-8.5 m during the MRE, we calculate a range of paleoearthquake magnitudes of M_w 7.64-7.69. Applying these same regressions for our penultimate event yields a paleoearthquake magnitude of M_w 7.54-7.59. Using the slightly modified empirical equations of Biasi and Weldon (2006), we calculate estimated paleoearthquake magnitudes of M_w 7.91-7.98 for the MRE and M_w 7.76-7.84 for the penultimate event. These paleo-event magnitudes are similar to those estimated by Hubbard et al. (2014) using slip values based on the uplifted marine terraces measured at Pitas Point, ~15 km west of the Day Road site.

Calculating paleo-earthquake magnitudes based on rupture area-to-magnitude regressions (rather than slip-to-moment-magnitude) allows us to speculate on the potential maximum magnitudes for earthquakes involving the Ventura fault. Using the empirical relationships discussed in Wells and Coppersmith (1994) and Hanks and Bakun (2002; 2008), we have estimated rupture magnitudes for several multi-segment rupture scenarios. These paleoearthquake magnitudes are recorded in Table 3.

As noted by Hubbard et al. (2014), rupture of just the Ventura fault can produce an earthquake of M_w 6.07-6.21. With the inclusion of the Pitas Point fault, fault rupture area increases significantly from 122 km^2 to 446.2 km^2 and the magnitude estimates increase to M_w 6.63-6.71. Including the downdip blind thrust portion of the Ventura fault identified by Hubbard et al. (2014) further increases the rupture area and thus the potential earthquake magnitude to M_w7.04-7.09. A system-wide rupture involving the Ventura, Pitas Point, and San Cayetano faults together with the deeper blind thrust ramp has the potential to produce a M_w 7.28-7.45 earthquake. An upper bound of magnitudes can be estimated using displacements recorded by the uplifted terraces at Pitas Point (Rockwell et al., 2011); the 8-10 m uplift events observed at the site along the crest of the Ventura Avenue Anticline suggest an earthquake magnitude up to M_w 8.1 (Hubbard et al., 2014).

An additional consideration in determining paleomagnitude estimates for past ruptures on the Ventura fault is the structural position of the Day Road transect along the thrust system. The eastern end of the Ventura fault, ~3 km east of the Day Road site, forms a "soft", en echelon segment boundary with the southern San Cayetano fault to the east. Thus, the reverse displacements we calculate from paleo-uplift events at Day Road may underestimate the average displacement of a multi-segment rupture involving the entire length of the Pitas Point-Ventura fault-southern San Cayetano fault system. This implies that our results are compatible with the larger paleo-event estimates.

4.6 Implications for seismic hazard in southern California

From a seismic hazard assessment standpoint, one of the most important issues concerning the faults of the western Transverse Ranges is the size of future earthquakes that they might produce. As described above, the large vertical uplift events that occurred during the past two earthquakes observed at Day Road indicate very large thrust displacements on the order of 5.5 to ≥8.5 m, despite the fact that this study site is only a few kilometers from the eastern end of the Ventura fault. The seismogenic potential of the Ventura fault has been debated for some time (Sarna-Wojcicki et al., 1976; Sarna-Wojcicki and Yerkes, 1982; Yeats, 1982; Huftile and Yeats, 1995). The persistent disagreement on this matter stems from the uncertainty of the fault geometry at depth. The new 3D model of Hubbard et al (2014) confirms that the Ventura fault extends to seismogeneic depth, and hypothesizes connectivity of the Ventura, San Cayetano and Red Mountain faults that might allow for large-magnitude, multi-segment ruptures in the western Transverse Ranges. Specifically, the Ventura fault forms the middle section of a >200-km-long, east-west belt of large, discrete, yet interconnected reverse and oblique-slip faults that extends across the western and central Transverse Ranges.

Although each individual fault in the Transverse Ranges fault system represents a major seismic source in its own right, a system-wide, multi-segment rupture involving the Ventura fault together with other major faults of the western Transverse Ranges could cause catastrophic damage to the densely urbanized areas of the Ventura and Los Angeles basins. One of the largest of these potential multi-fault earthquakes involves rupture of the rapidly slipping eastern San Cayetano fault westward via the blind, southern San Cayetano fault, onto the blind Ventura thrust fault together with correlative faults to the west (e.g., Lower Pitas Point fault; Figure 1). Such a 75- to 100 km-long multi-segment rupture could potentially encompass a fault-plane area of as much as several thousand square kilometers – similar to the rupture area of the great 1857 M_w 7.8 Fort Tejon and 1906 M_w 7.9 San Francisco earthquakes on the San Andreas fault. To the east, potential subsurface connectivity of the San Cayetano fault with the Santa Susana and

Sierra Madre faults may provide a mechanism to extend the ruptures further eastward, but this subsurface structure remains poorly understood.

Unfortunately, there are few historical and paleoseismic data available to test the validity of the various rupture scenarios. No large-M_w (M>7) earthquakes have occurred on any of the faults surrounding the Ventura basin for at least 200 years, suggesting the possibility that recurrence intervals for these faults are relatively long and that they may therefore rupture in larger, multi-segment events. The most recent potentially large-magnitude earthquake in the Ventura region occurred on December 21, 1812. Toppozada et al. (1981) originally suggested that this earthquake was generated by rupture of an offshore fault beneath the Santa Barbara Channel. Toppozada et al. (2002), however, subsequently speculated that this earthquake may have occurred on the western Big Bend section of the San Andreas fault, effectively extending the December 8, 1812 San Andreas fault Mojave segment rupture to the northwest. There is no direct evidence, however, that the second 1812 earthquake occurred on the San Andreas fault, and felt intensity reports are consistent with a western Transverse Ranges source. Dolan and Rockwell (2001) documented a large-displacement (>~5 m) thrust event on the eastern San Cayetano fault sometime after 1660 AD. If this event was not the December 21, 1812 earthquake, then it occurred between 1660 AD and the beginning of the historic period, which likely began in the 1780s for an earthquake of this size (Dolan and Rockwell, 2001).

The limited slip-per-event data that are available from the Ventura-Pitas Point fault suggest that large magnitude earthquakes may have indeed occurred along these and related faults. Specifically, Rockwell (2011) and Hubbard et al., (2014) point out four paleo-shore faces along the Ventura coastline at Pitas Point that they argue were uplifted 5-10 m in each of the four most recent events. Uplift of these shore faces at the Pitas Point site, which lies along the structural crest of the VAA, occurred during earthquakes at ~800-1,000 years ago for the MRE, ~1,900 years ago for the penultimate event, ~3,500 years ago for Event 3, and ~5,000 years ago for Event 4. Uplifts of this magnitude would require large (M_w7.6-8.0) earthquakes (Biasi and Weldon, 2006), likely rupturing a fault area equivalent to the entire Ventura-Pitas Point fault combined with other faults to the east and west (e.g., San Cayetano fault and western Santa Barbara Channel faults [Hubbard et al., 2014]). The similarity in age between the post-800±100-year-old most recent event at Day Road and the ~800- to 1,000-year-old MRE at Pitas Point based on uplifted marine terraces (Rockwell, 2011; Hubbard et al., 2014) suggests that these sites may both record the same event. We reiterate that the Day Road site is only ~3 km from the eastern end of the well-defined Ventura fault fold scarp, and that slip in this area is gradually transferred eastward from the Ventura fault onto the southern San Cayetano fault across a “soft” segment boundary. Thus, the large displacement that occurred during the MRE at Day Road (7.3-8.5 m) close to the eastern end of the Ventura fault strongly suggests that the MRE rupture continued eastward onto the southern San Cayetano fault.

Alternatively, the age data and the absence of sedimentary growth above the current topographic scarp leave open the possibility that the “MRE” at Day Road actually represents more than one event. For example, if the post-1660 AD surface rupture with 5 m of reverse displacement observed by Dolan and Rockwell (2001) on the eastern San Cayetano fault 40 km east of Ventura was not the December 21, 1812 earthquake, then this event could conceivably be recorded as part of the MRE at Day Road. The post-1660 AD eastern Can Cayetano fault event, however, is not observed at Pitas Point, demonstrating that if this scenario is correct, the eastern San Cayetano and Ventura fault rupture did not extend as far west as Pitas Point.

The penultimate event observed at Pitas Point (~1.9 ka; Rockwell, 2011) does not appear to have produced any detectable paleo-earthquake signal on the Ventura fault at the Day Road site, as this date falls within the middle of the c. 800- to 3,000-year-old stratigraphic section, which does not change thickness across the fold, thus indicating that it was deposited during a period of structural quiescence. This observation suggests that at least sometimes the Ventura-Pitas Point system does not rupture in its entirety. The fault may rupture partial segments in smaller events at times between the multi-segment ruptures. The similarity in uplift height (and presumably magnitude) during each of the past four uplift events at Pitas Point, however, suggests that each event records a similar-sized rupture. Thus, it seems unusual for only Event 2 to not have ruptured as far East as Day Road. One possible alternative scenario may involve the rupture of both the Pitas Point fault and the San Cayetano fault with slip transferred eastward along the deep, blind thrust ramp and southern San Cayetano fault, bypassing the shallower part of the easternmost Ventura fault.

The base of the growth interval in the penultimate uplift event at Day Road is ~5 ka, suggesting that at least the lower part of the Unit C growth interval at Day Road was deposited in response to the 4th event at Pitas Point, which occurred ~5 ka. The top of the growth interval at Day Road is ~3 ka, which is ~500 years younger than the age of the 3rd event at Pitas Point documented by Rockwell (2011) and Hubbard et al., (2014), suggesting that the Day Road growth interval may encompass both the 3rd and 4th events observed at Pitas Point. If so, the >4.5m of growth observed at Day Road records uplift during two events. If correct, this inference would indicate that displacements in the scarp-forming events observed at Day Road were likely much smaller than those during the MRE. Alternatively, the entire >4.5 m uplift may have occurred during Pitas Point event 4 c. 5 ka, with Pitas Point event 3 either bypassing the eastern

Ventura fault, as discussed above for the Day Road penultimate event, or being located further west along the thrust system.

5 Conclusions

Results from newly acquired high-resolution seismic reflection data, borehole cores, CPTs, and luminescence and radiocarbon geochronology along the Day Road profile reveal evidence for folding events that we interpret as due to large-magnitude earthquakes on the underlying Ventura fault. The most recent event, which occurred soon after deposition of pre-event strata dated at c.1100–1300 AD, generated the 6-m-high fold scarp observed at our Day Road study site in eastern Ventura. The prominent surface scarp is underlain by a 4-m thick, post-3 ka sequence of alluvial fan strata that do not change thickness across the fold scarp, indicating that they were folded in the MRE and that the surface scarp records uplift during that event. The penultimate event(s) at this site is recorded by a southward-thickening interval of sedimentary growth strata that onlapped a now-buried, >4.5-m-tall fold scarp that formed between 3-5 ka. This growth interval is underlain by a ~5 m thick section spanning 5-9 ka that does not change thickness across the fold, indicating that this was a period of structural quiescence. The very large reverse displacements required to generate the 4.5-6 m uplifts in the two most recent earthquakes require that these were large magnitude events likely well in excess of M_w 7, and potentially approaching M_w 8. Comparison of our paleoearthquake ages and displacements with similar data generated by Rockwell (2011) and Hubbard et al., (2014) from uplifted paleo-shorelines at Pitas Point 15 km to the west along the structural crust of the Ventura Avenue Anticline indicates that; (1) the post-c. 1100–1300 AD MRE overlaps with the age of the MRE at Pitas Point (c. 1000–1200 AD), suggesting that these sites recorded the same earthquake; (2) the c. 1.9 ka penultimate event at Pitas Point did not extend through the Day Road site on the eastern Ventura fault, indicating that these sites do not always rupture together despite being on the same fault system 15 km apart; and (3) the 3-5 ka growth interval at Day Road overlaps with the 3.5 ka and 5 ka 3rd and 4th events documented at Pitas Point, suggesting that these two events may have spanned the entire Ventura-Pitas Point fault system. The very large displacement in the MRE at Day Road indicated by 6 m of uplift is slightly smaller than the 8-9 m of uplift recorded in the MRE at Pitas Point, which lies near the structural crest of the VAA. The Day Road site, however, lies close to the eastern end of the Ventura-Pitas Point fault system, and such large displacements suggest that this rupture may have extended eastward from the Ventura fault across the en echelon left step between the Ventura fault and the southern San Cayetano fault to the east. In contrast, the ≥ 4.5 m of 3-5 ka sedimentary growth observed at Day Road is much smaller than the 8-10 m uplifts observed in the 3rd and 4th events at Pitas Point. Thus, if the Day Road growth section does record both the 3rd and 4th events at Pitas Point, these events must have had much smaller displacements than observed to the west. Together with the observation that the penultimate event at Pitas Point does not appear to have extended through the Day Road site, these observations point to complex patterns of earthquake rupture on the Ventura fault during the mid- to late Holocene. The large displacements observed, however, particularly in the MRE, indicate that these were large-magnitude events that likely involved multi-segment ruptures that connected multiple faults in the western Transverse Ranges. The recurrence of such large-magnitude events has critically important implications for seismic hazard assessment in southern California. Specifically, the occurrence of large thrust fault earthquakes adjacent to the deep (> 10 km) Ventura basin would cause significant amplification of seismic waves, leading to damaging ground motions over much of the region, perhaps extending into the Los Angeles metropolitan area, the San Fernando basin, and the San Gabriel Valley. Moreover, large-displacement ruptures of the Ventura fault along its offshore western continuation, the Pitas Point fault, could potentially generate significant tsunamis near the coast, limiting potential warning times. It is worth noting, however, that the relatively shallow water depths at the fault-sea floor interface will reduce the overall magnitude of the water mass involved in any such tsunamis. The recurrence intervals for the large-magnitude Ventura fault earthquakes documented at our Day Road site are significantly longer than those for the recurrence of “Big Ones” on the San Andreas fault system, with inter-event times measurable in thousands of years, rather than hundreds. Nevertheless, the potential magnitude of multi-segment western Transverse Ranges earthquakes involving the Ventura fault may approach those of San Andreas earthquakes, indicating that it is crucial that the prospects for the recurrence of large magnitude, multi-segment earthquakes on the Ventura and mechanically interconnected faults in the western and central Transverse Ranges be properly considered in future regional seismic hazard assessments.

References

Biasi, G.P., and Weldon II, R.J., 2006, Estimating surface rupture length and magnitude of paleoearthquakes from point measurements of rupture displacement: Seismological Society of America Bulletin, v. 96(5), p. 1612-1623.

Brown, N.D., Rhodes, E.J., Antinao, J.L., and McDonald, A.E., in revision for publication, Single-grain post-IR IRSL signals of K-feldspars from alluvial fan deposits in Baja California Sur, Mexico: submitted to Quaternary International.

Buylaert, J.P., Murray, A.S., Thomsen, K.J., and Jain, M., 2009, Testing the potential of an elevated temperature IRSL signal from K-feldspar: Radiation Measurements, v. 44, p. 560-565.

Buylaert, J.P., Jain, M., Murray, A.S., Thomsen, K.J., Thiel, C., and Sohbati, R., 2012, A robust feldspar luminescence dating method for Middle and Late Pleistocene sediments: Boreas, v. 41, p. 435-451. DOI:10.1111/j.1502-3885.2012.00248.x

Dolan, J.F., Sieh, K., Rockwell, T.K., Yeats, R.S., Shaw, J., Suppe, J., Huftile, G.J., and Gath, E.M., 1995, Prospects for Larger or More Frequent Earthquakes in the Los Angeles Metropolitan Region: Science, v. 267, p. 199-205.

Dolan, J.F., and T. Rockwell, T.K., 2001, Paleoseismic evidence for a very large (Mw >7), post-A.D. 1660 surface rupture on the eastern San Cayetano Fault, Ventura County, California; was this the elusive source of the damaging 21 December 1812 earthquake?: Seismological Society of America Bulletin, v. 91(6), p. 1417-1432.

Donnellan, A., Hager, B.H., and King, R.W., 1993a, Rapid north-south shortening of the Ventura basin, southern California: Nature, v. 366, p. 333-336.

Donnellan, A., Hager, B.H., King, R.W., and Herring, T.A., 1993b, Geodetic measurement of deformation in the Ventura basin, southern California: Journal of Geophysical Research, v. 98, p. 21727-21739.

Hager, B.H., Lyzenga, G.A., Donnellan, A., and Dong D., 1999, Reconciling rapid strain accumulation with deep seismogenic fault planes in the Ventura basin, California: Journal of Geophysical Research, v. 104(B11), p. 25,207-25,219.

Hanks, T.C., and Bakun, W.H., 2002, A bilinear source-scaling model for M-logA observations of continental earthquakes: Seismological Society of America Bulletin, v. 92, p. 1841-1846.

Hanks, T.C., and Bakun, W.H., 2008, M-log A observations of recent large earthquakes: Seismological Society of America Bulletin, v. 98, p. 490-494.

Hornafius, J.S., Luyendyk, B.P., Terres, R.R., and Kamerling, M.J., 1986, Timing and extent of Neogene tectonic rotation in the western Transverse Ranges, California: Geological Society of America Bulletin, v. 97, p. 1476-1487, doi: 10.1130/0016-7606(1986)97<1476:TAEONT>2.0CO;0.

Hubbard, J., Shaw, J.H., Dolan, J., Pratt, T.L., McAuliffe, L., and Rockwell, T.K., 2014, Structure and seismic hazard of the Ventura Avenue anticline and Ventura fault, California: Prospect for large, multi-segment ruptures in the Western Transverse Ranges: Seismological Society of America Bulletin, v. 104, p. 1070-1087.

Huftile, G.J., and Yeats, R.S., 1995a, Convergence rates across a displacement transfer zone in the western transverse ranges, Ventura Basin, California: Journal of Geophysical Research, v. 100, p. 2043-2067.

Jackson, J., and Molnar, P., 1990, Active Faulting and Block Rotations In The Western Transverse Ranges, California: Journal of Geophysical Research, v. 95, p. 22,073-22,087.

Jain, M. and Ankjærgaard, C., 2011, Towards a non-fading signal in feldspar: insight into charge transport and tunnelling from time-resolved optically stimulated luminescence: Radiation Measurements, v. 46, p. 292–309.

Luyendyk, B.P., Kamerling, M.J., Terres, R.R., and Hornafius, J.S., 1985, Simple shear of southern California during the Neogene: Journal of Geophysical Research, v. 90, p. 12454-12466.

Luyendyk, B.P., 1991, A model for Neogene crustal rotations, transtension, and transpression in southern California: Geological Society of America Bulletin, v. 103, p. 1528-1536.

Marshall, S.T., Cooke, M.L., and Owen, S.E., 2008, Effects of non-planar fault topology and mechanical interaction on fault slip distributions in the Ventura Basin, CA: Seismological Society of America Bulletin, v. 98(3), p. 1113-1127, doi:10.1785/0120070159.

McAuliffe, L.J, 2014, Paleoseismologic and slip rate studies of three major faults in southern California: Understanding the complex behavior of plate boundary fault systems over millennial timescales [Ph.D. dissertation]: University of Southern California, Los Angeles, 294 p.

Novoa, E., Suppe, J., and Shaw, J.H., 2000, Inclined-shear restoration of growth folds: American Association of Petroleum Geologists Bulletin, v. 84, p. 787-804.

Ogle, B.A. and Hacker, R.N., 1969, Cross section coastal area Ventura County, in Geology and Oil Fields of Coastal Areas, Ventura and Los Angeles Basins, California: Pacific Section AAPG, SG, and SEPM, 44th Annual Meeting Field Trip, Guidebook.

Perry, S.S., and Bryant, W.A., 2002, Fault number 91, Ventura fault, in Quaternary fault and fold database of the United States. U.S. Geological Survey website: http: //earthquakes.usgs.gov/regional/qfaults (accessed May 2011).

Peterson, M.D., and Wesnousky, S.G., 1994, Fault slip rates and earthquake histories for active faults in southern California: Seismological Society of America Bulletin, v. 84(5), p. 1608–1649.

Rockwell, T. K., 1983, Soil chronology, geology, and neotectonics of the north central Ventura Basin, California [Ph.D. dissertation]: University of California, Santa Barbara, 424 p.

Rockwell, T., 1988, Neotectonics of the San Cayetano fault, Transverse Ranges, California: Geological Society of America Bulletin, v. 100, p. 500-513.

Rockwell, T., 2011, Large Co-Seismic Uplift of Coastal Terraces Across the Ventura Avenue Anticline: Implications for the Size of Earthquakes and the Potential for Tsunami Generation, 2011 SCEC annual meeting Plenary Session III

Rhodes, E. J., in review, Dating sediments using potassium feldspar single-grain IRSL: initial methodological considerations: Quaternary International.

Sarna-Wojcicki, A.M., Williams, K.M., and Yerkes, R.F., 1976, Geology of the Ventura Fault, Ventura County, California. U.S. Geological Survey Miscellaneous Field Studies, map MF-781, 3 sheets, scale 1:6,000.

Sarna-Wojcicki, A.M., and Yerkes, R.F., 1982, Comment on article by Yeats, R.F., entitled "Low-shake faults of the Ventura Basin, California", in Neotectonics in Southern California, Cooper, J.D., eds., Geological Society of America, 78th Cordilleran Section Annual Meeting, Guidebook, 17-19.

Scientists of the U.S. Geological Survey and the Southern California Earthquake Center, 1994, The Magnitude 6.7 Northridge, California, earthquake of 17 January 1994: Science, v. 266, p. 389-397, doi:10.1126/science.283.5407.1516.

Stein, R.S., and Yeats, R.S., 1989, Hidden earthquakes: Scientific American, p. 48-57.

Stuiver, M., and Polach, H., 1977, Reporting of ^{14}C data: Radiocarbon, v. 19, p. 355–363.

Thiel, C., Buylaert, J., Murray, A., Terhorst, B., Hofer, I., Tsukamoto, S., and Frechen, M., 2011, Luminescence dating of the Stratzing loess profile (Austria) – Testing the potential of an elevated temperature post-IR IRSL protocol: Quaternary International, v. 234, p. 23-31.

Toppozada, T.R., Real, C.R., and Parke, D.L., 1981, Preparation of isoseismal maps and summaries of reported effects for pre-1900 California earthquakes: California Division of Mines and Geology Open-File Rept. 81-11.

Toppozada, T.R., Branum, D.M., Reichle, M.S., and Hallstrom, C.L., 2002, San Andreas fault zone, California: M>5.5 earthquake history: Seismological Society of America Bulletin, v.92, p. 2555-2601.

Wells, D. L., and K. J. Coppersmith, 1994, New empirical relationships among magnitude, rupture length, rupture width, rupture area, and surface displacement: Seismological Society of America Bulletin, v. 84, p. 974-1002.

WGCEP (Working Group on California Earthquake Probabilities), 1995, Seismic hazards in southern California: probable earthquakes, 1994 to 2024: Seismological Society of America Bulletin, v. 85, p. 379-439.

Yeats, R.S., 1982, Low-shake faults of the Ventura basin, California, in Cooper, J.D. ed., Neotectonics in Southern California: Geological Society of America, 78th Cordilleran Section Annual Meeting, Guidebook, p. 3-15.

Yeats, R.S., 1983, Large-scale Quaternary detachments in Ventura basin, southern California: Journal of Geophysical Research, v. 88, p. 569-583.

4.9 Figure Captions

Figure 1. Location map showing major faults and folds in the western Transverse Ranges. The darker shaded region outlines the surface extent of the Ventura basin. Selected cities are identified with green circles. The Pitas Point fault is the offshore continuation of the Ventura fault. Blue lines show high resolution seismic reflection profiles along Day Road (west) and Brookshire Avenue (east). The blind southern San Cayetano fault has been interpreted by Hubbard et al. (2014) as having two possible geometries: Green line shows location of south-facing fold scarp associated with slip on the southern San Cayetano fault. Borehole and high-resolution seismic reflection from across this scarp reveal an active synclinal axial surface suggesting that this scarp is caused by a south-dipping backthrust off the main north dipping blind thrust ramp (Hubbard et al., 2014) Red dashed line in one possible vertical projection of

the tipline at the top of this backthrust. Black inset box shows location of geologic map (Supplementary figure S1). Figure modified from Hubbard et al., 2014.

Figure 2. 3D perspective view of the western Ventura basin illustrating the relationship between the Ventura fault, the Ventura Avenue Anticline and the other major faults in the western Transverse Ranges. Solid blue line shows location of the Day Road and Brookshire Avenue transects. Figure modified from Hubbard et al., 2014

Figure 3. Eastward-looking perspective view of Day Road high-resolution seismic reflection profile (red line; see data repository figure S3), and continuously cored borehole (yellow ovals) and CPT (green ovals) locations along the Day Road transect using a GoogleEarth base image with 3x vertical exaggeration to highlight the south-facing Ventura fault scarp (orange swath). Red squares show locations of two sampling pits used to constrain the age of the most recent earthquake on the Ventura fault at this location. These are shown as being west of the sampling transect for clarity; both pits were located along the western edge of Day Road ~3m west of the borehole-CPT transect.

Figure 4. Northward-looking oblique aerial view showing location of high-resolution seismic reflection profile (red line), continuously cored boreholes (yellow ovals), and CPTs (green ovals) along the Day Road transect. Base image is from GoogleEarth, shown with 3x vertical exaggeration. The prominent east-west fold scarp associated with the underlying Ventura fault is shown with the orange swath. Extent of the active Holocene Arroyo Verde alluvial fan is highlighted by the blue shading.

Figure 5. High-resolution seismic reflection profile at Brookshire Avenue. Black dashed line shows projected synclinal axial surface associated with the underlying blind Ventura fault. Upper image shows local topography with 5x vertical exaggeration. Dashed green line S1 shows active synclinal axial surface and dashed red line A1 shows active anticlinal axial surface. Figure Modifies from Hubbard et al. (2014).

Figure 6. Cross-section of the Day Road transect showing major stratigraphic units (3x vertical exaggeration). Individual borehole and CPT logs are not shown. Black vertical lines are continuously cored boreholes and red vertical lines are CPT data. Green horizontal line is the present day topography. Colors denote different sedimentary units. See supplementary figure S6 for version of this figure that includes detailed sediment grain size and color data from boreholes and CPTs. Red vertical arrows on the right show intervals of topographic and stratigraphic growth indicative of discrete uplift events. Green vertical arrows show no-growth intervals. Black horizontal lines along the top of the profile show the far field topographic slope of the Arroyo Verde alluvial fan at the site. Yellow stars indicate locations of charcoal samples and pink hexagons show locations of luminescence samples. Letter b indicates location of burn markings found on small pebbles. The topographic profile was taken from measured GPS readings in the field at every shotpoint (4 m spacing).

Figure 7. Stratigraphic column showing projected locations of luminescence and ^{14}C sample ages on to borehole DY-4.

Table 1. Radiocarbon and luminescence ages and calibrated, calendric dates of samples from the Day Road transect. Projected depth to borehole DY-4 are estimates.

Table 2. Uplift, along fault displacement, age limits, and estimated moment magnitude (M_w) for the two paleoearthquakes on the Ventura fault from Day Road borehole and CPT results.

Table 3. Earthquake magnitude estimates based on rupture area to magnitude regressions.

Supplementary figure S1. Geologic map of the Ventura area showing fold scarp associated with the underlying Ventura fault (red polygon), locations of 2D high-resolution seismic reflection profiles (blue lines) and borehole/CPT locations (green and yellow circles). The Day Road transect is the only line that transcends a late Holocene active alluvial fan. The black dotted overlay shows the built up area of the city of Ventura. Map modified from Sarna-Wojcicki et al., (1976).

Supplementary figure S2. Location map showing high-resolution seismic reflection transects through the city of Ventura.

Supplementary figure S3. High-resolution seismic reflection profile at Day Road. Black dashed line shows projected synclinal axial surface associated with the underlying blind Ventura fault. Upper image shows local topography (5x vertical exaggeration) and locations of continuously cored boreholes (green) and CPTs (pink).

Supplementary figure S4. East wall of sampling pit DR-13. This pit is located on the downthrown side of the Ventura fault along the Day Road transect. This sampling pit was excavated adjacent to CPT-10. Locations of five luminescence samples are shown with yellow circles. Red lines show contacts between discrete stratigraphic units. Upper 1.5 feet of material is non-native fill.

Supplementary figure S5. (a) East wall of sampling pit DR-14. This pit is located on the upthrown side of the Ventura fault along the Day Road transect. This sampling pit was excavated 20 meters north of CPT-3. Locations of three luminescence samples are shown with yellow circles. Orange circle highlights location of charcoal sample DR14-CL01 from a depth of 126cm. Oblique black box shows projection of image b. Red line marks discrete contact between silty sand unit and the darker clay rich soil horizon below. (b) close up of sample locations. Orange circle shows location of charcoal sample DR14-CL01. The sediment surrounding the charcoal sample shows no signs of bioturbation.

Supplementary figure S6. Cross section of the Day Road transect showing major stratigraphic units and including detailed sediment grain size and color data from boreholes and CPTs. Black vertical lines are locations of continuously cored boreholes and red vertical lines are locations of CPT data. Green horizontal line is the present day topography (3x vertical exaggeration). Colors denote different sedimentary units. Red vertical arrows on the right side show regions of stratigraphic growth indicative of discrete uplift events. Green vertical arrows show no growth intervals. Black horizontal lines along the top of the profile show the far field topographic slope of the alluvial fan. Letter b indicates location of burn markings found on small pebbles. The topographic profile was taken from measured GPS readings in the field at every shotpoint (4 m spacing).

Figures

Figure 1

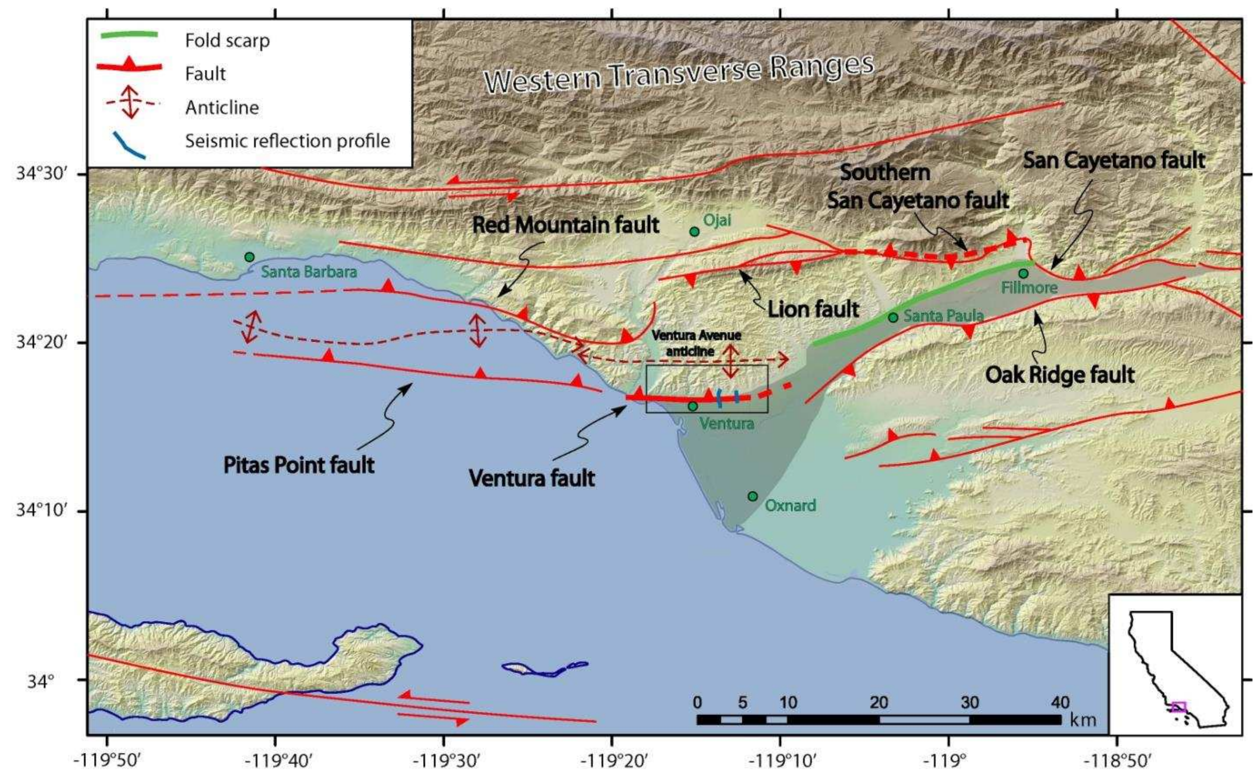

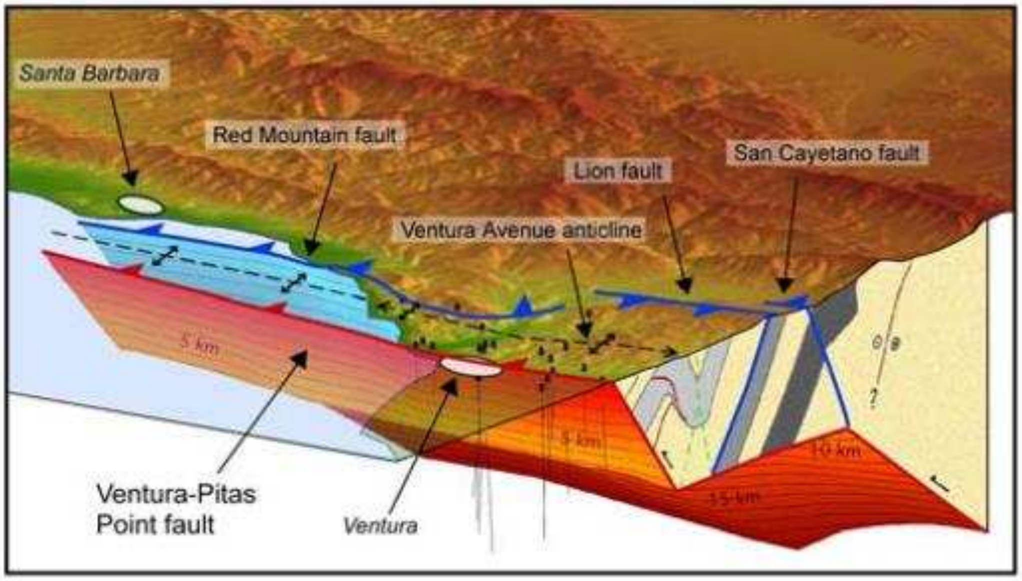
Santa Barbara
Red Mountain fault
Lion fault
San Cayetano fault
Ventura Avenue anticline
5 km
5 km
10 km
15 km
Ventura-Pitas
Point fault
Ventura

862

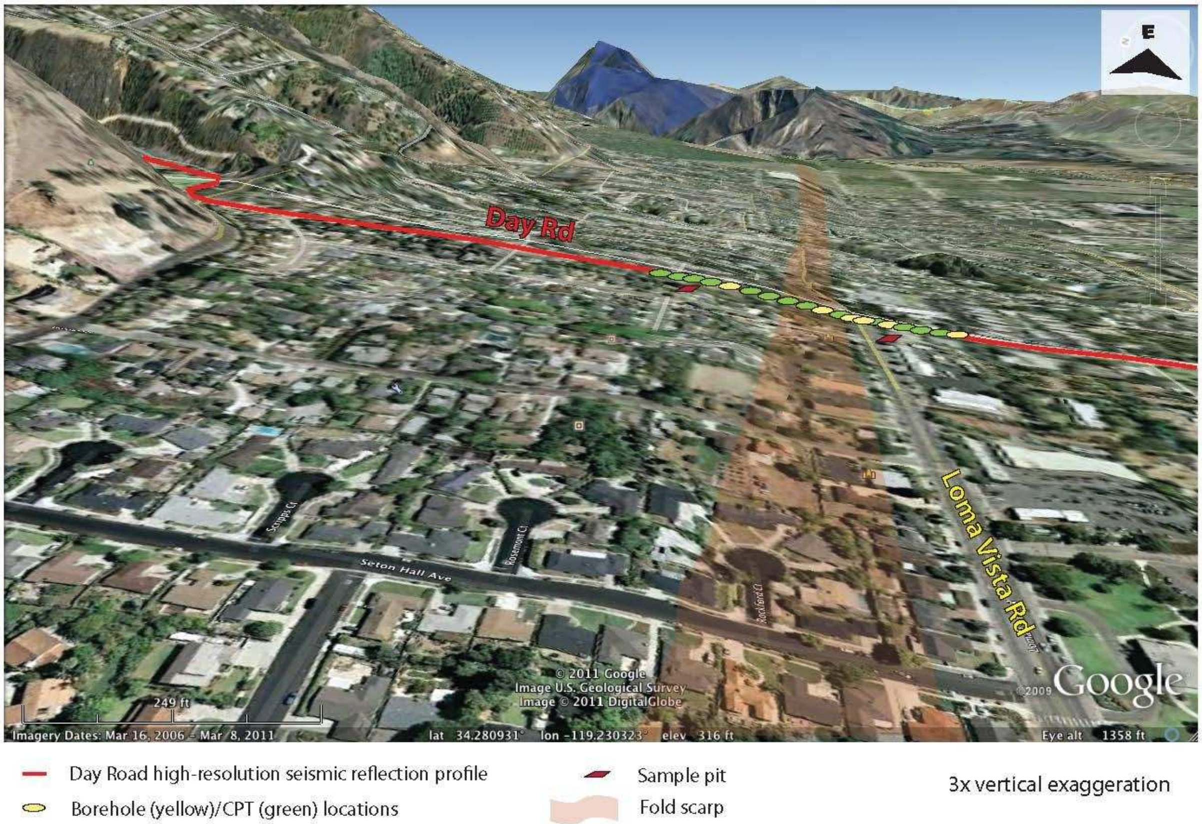
E
Day Rd
Loma Vista Rd
Seton Hall Ave
249 ft
© 2011 Google
Image U.S. Geological Survey
Image © 2011 DigitalGlobe
Imagery Dates: Mar 16, 2006 – Mar 8, 2011
Google
Day Road high-resolution seismic reflection profile
Borehole (yellow)/CPT (green) locations
Sample pit
Fold scarp
3x vertical exaggeration

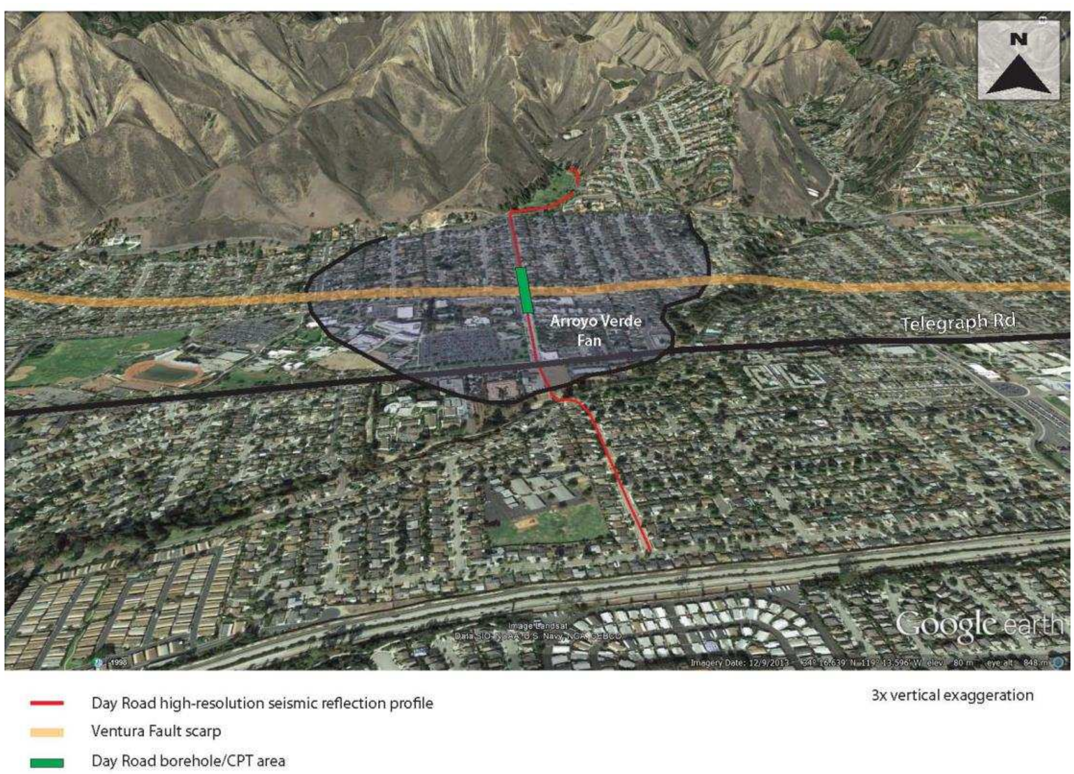
N
Arroyo Verde
Fan
Telegraph Rd
Google earth
Day Road high-resolution seismic reflection profile
Ventura Fault scarp
Day Road borehole/CPT area
3x vertical exaggeration

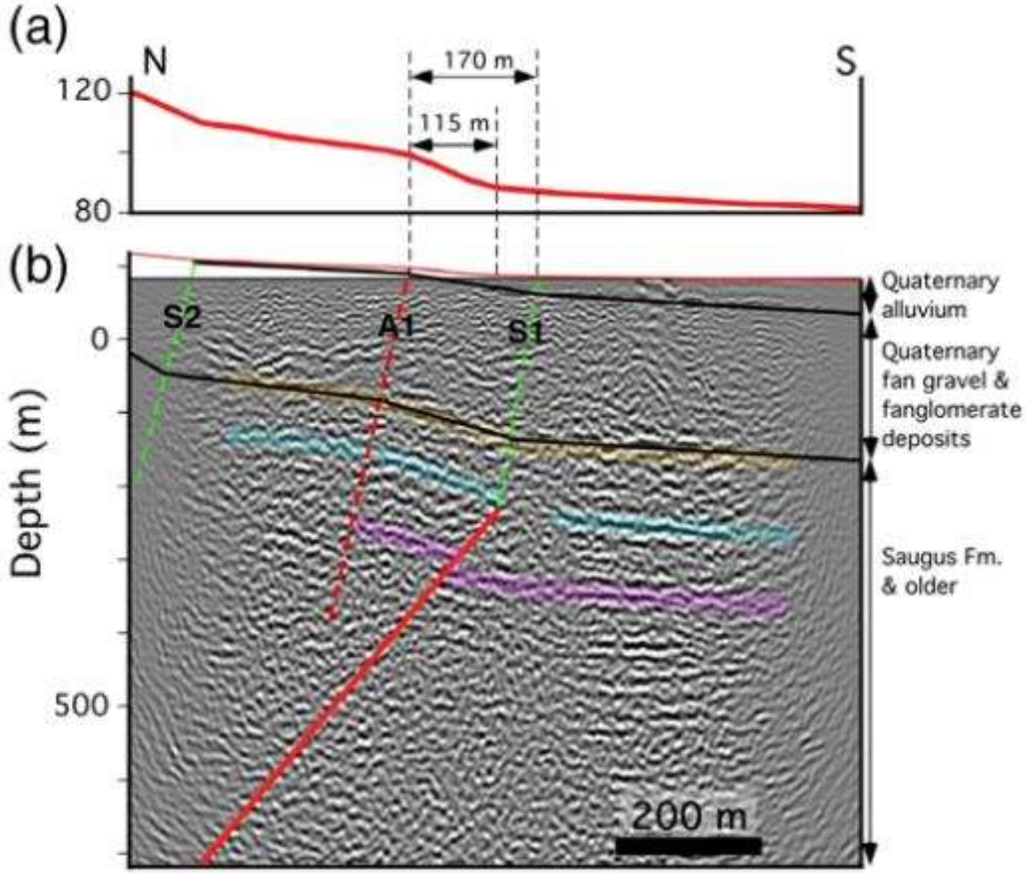
(a)
N
S
170 m
115 m
120
80
(b)
S2
A1
S1
0
500
Depth (m)
200 m
Quaternary alluvium
Quaternary fan gravel & fanglomerate deposits
Saugus Fm. & older

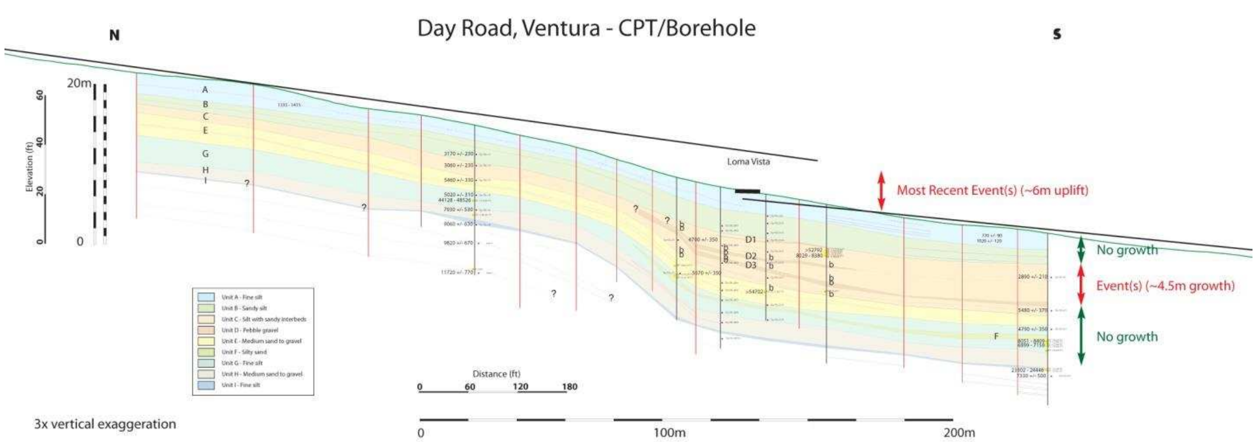
Day Road, Ventura - CPT/Borehole
N
S
Loma Vista
Most Recent Event(s) (~6m uplift)
No growth
Event(s) (~4.5m growth)
No growth
Distance (ft)
0
60
120
180
0
100m
200m
3x vertical exaggeration

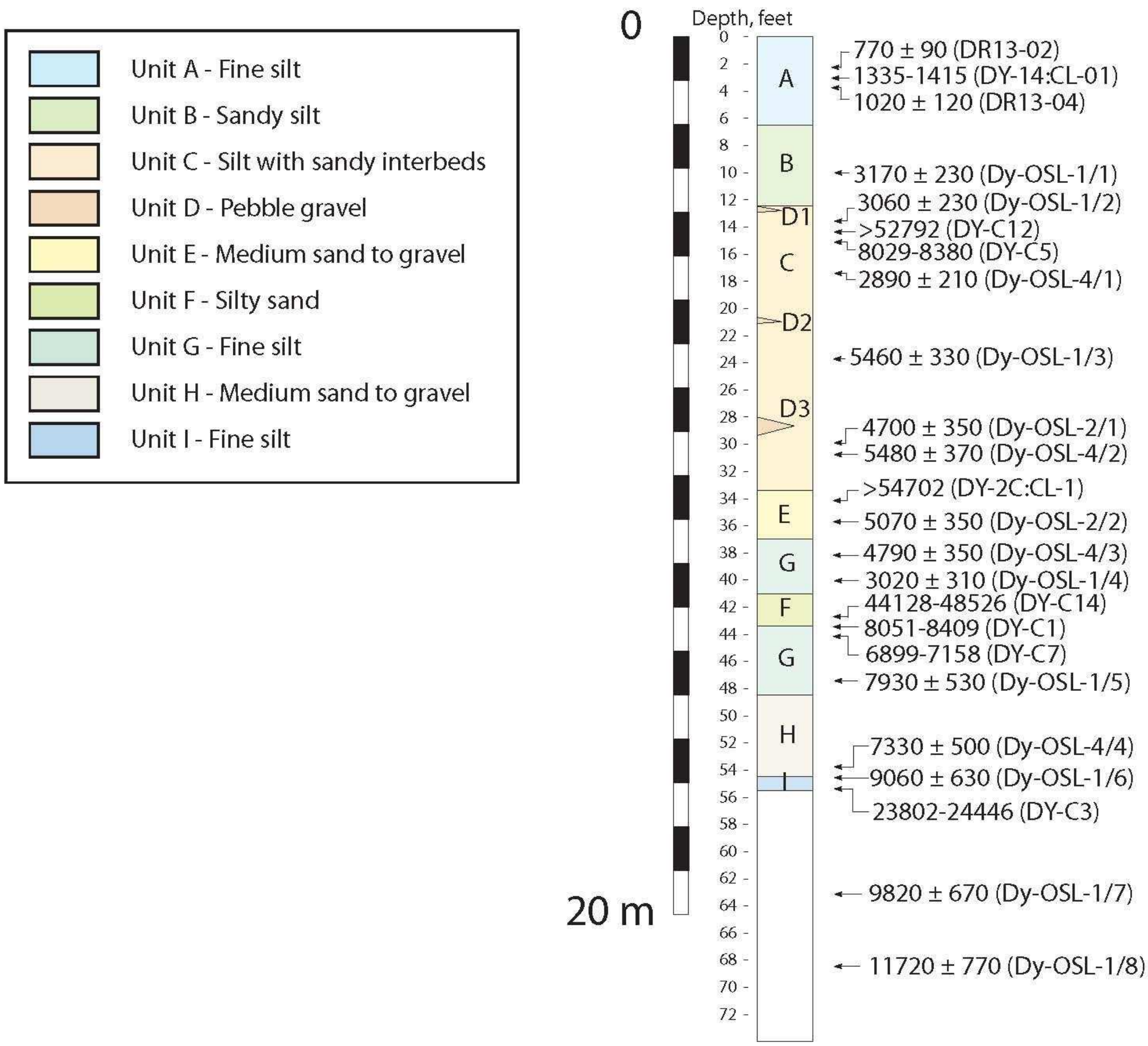

Supplementary Figures

Supplementary figure S1

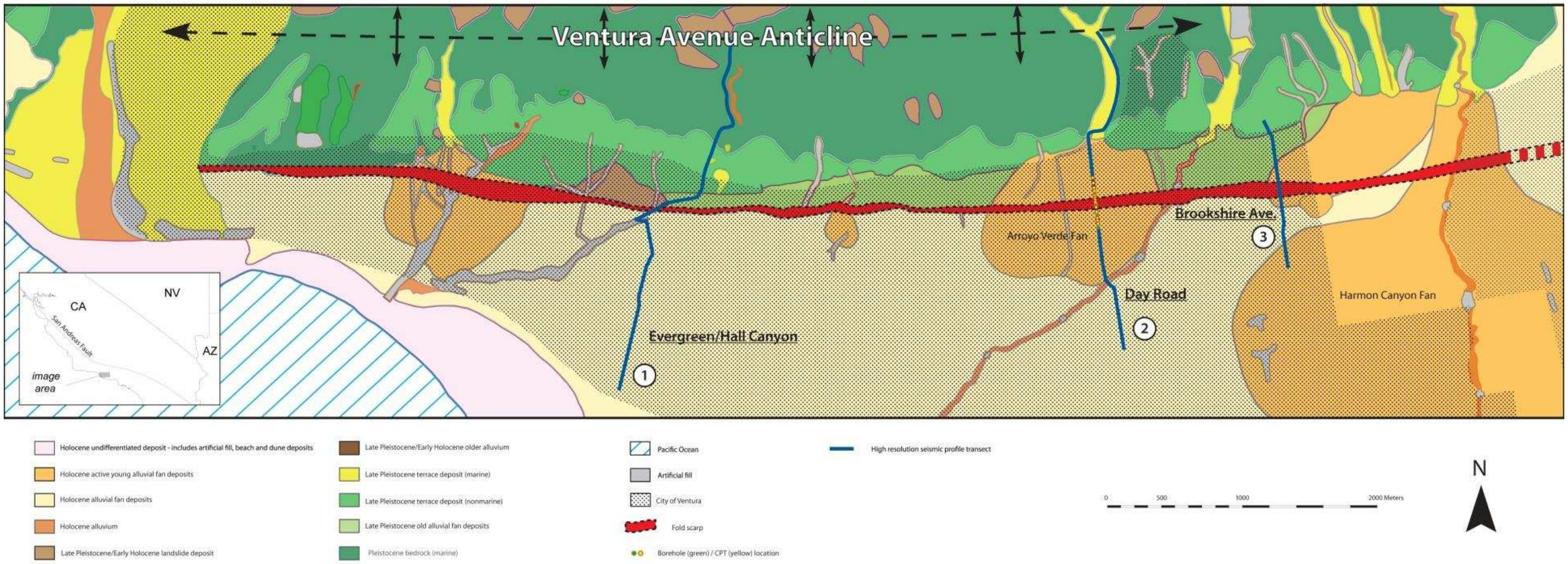

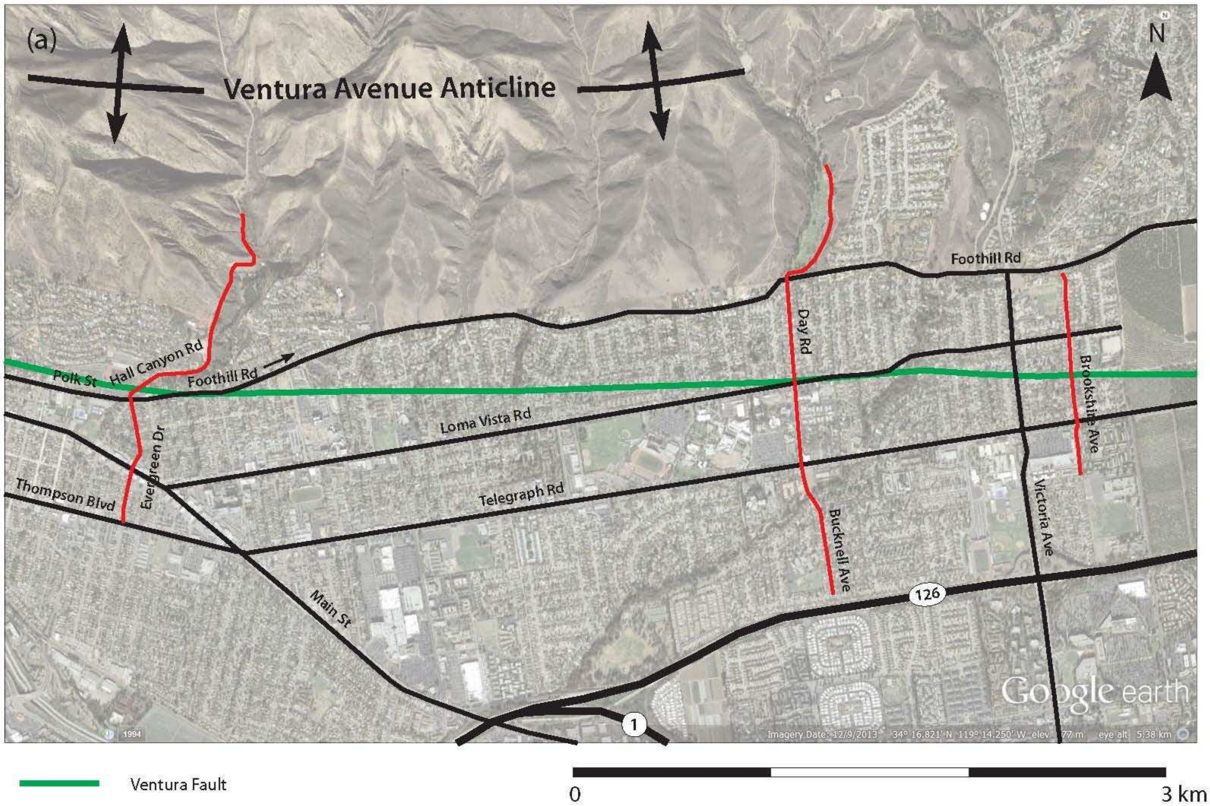
(a)
Ventura Avenue Anticline
N
Foothill Rd
Day Rd
Hall Canyon Rd
Polk St
Foothill Rd
Loma Vista Rd
Brookshire Ave
Evergreen Dr
Thompson Blvd
Telegraph Rd
Bucknell Ave
Victoria Ave
126
Main St
1
Google earth
Ventura Fault
0
3 km

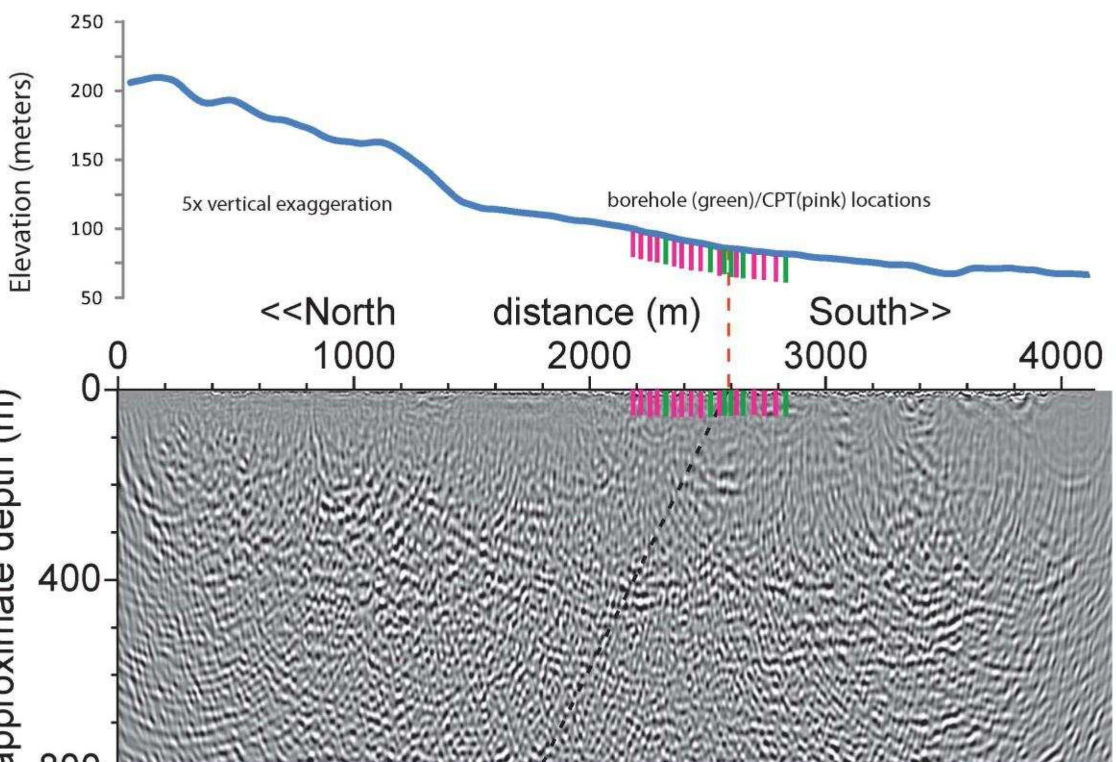
Elevation (meters)
250
200
150
100
50
5x vertical exaggeration
borehole (green)/CPT(pink) locations
<<North
distance (m)
South>>
0
1000
2000
3000
4000
approximate depth (m)
0
400
800

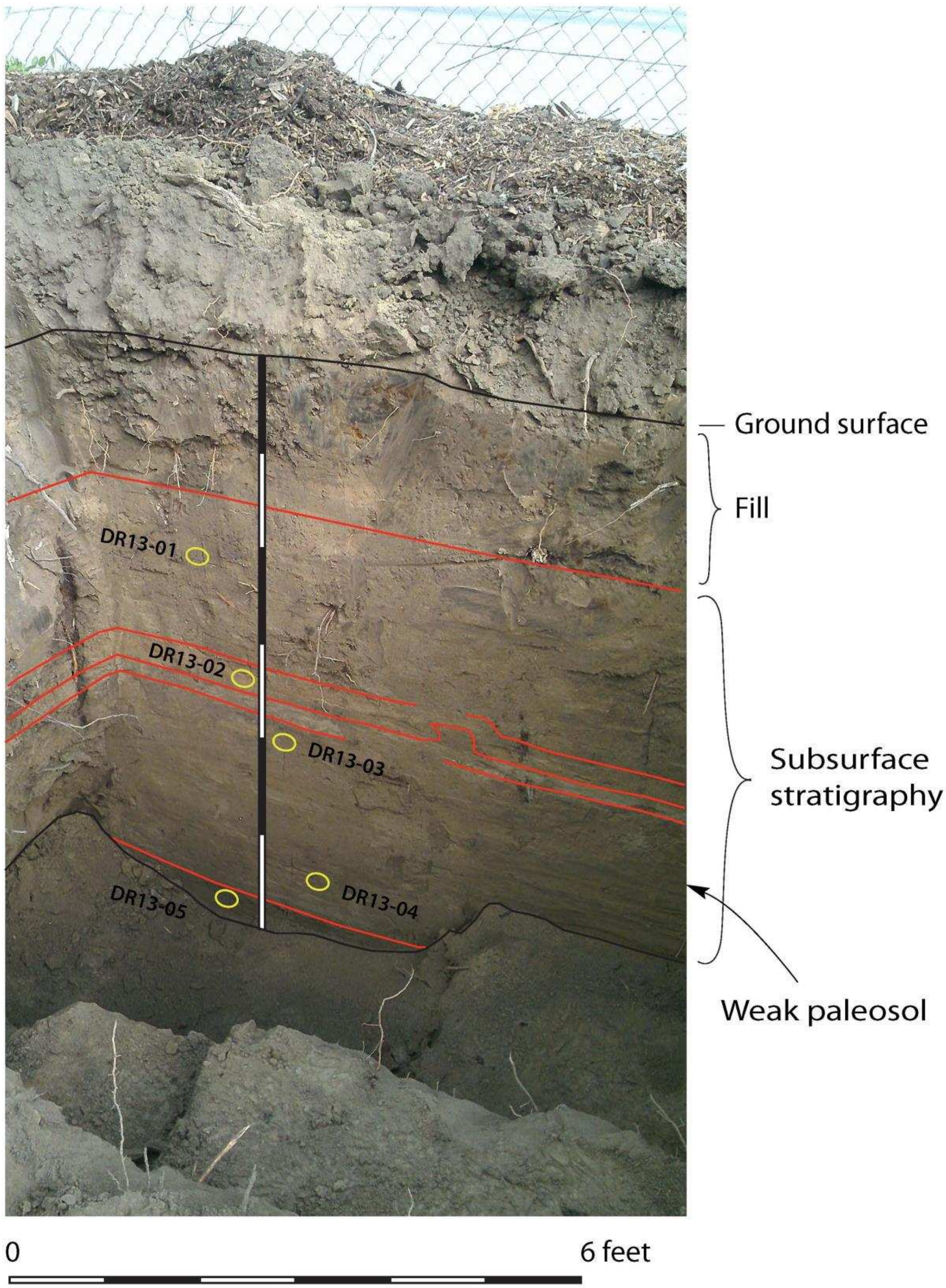

Ground surface
Fill
Subsurface stratigraphy
Weak paleosol
DR13-01
DR13-02
DR13-03
DR13-04
DR13-05
0
6 feet

Supplementary figure S3

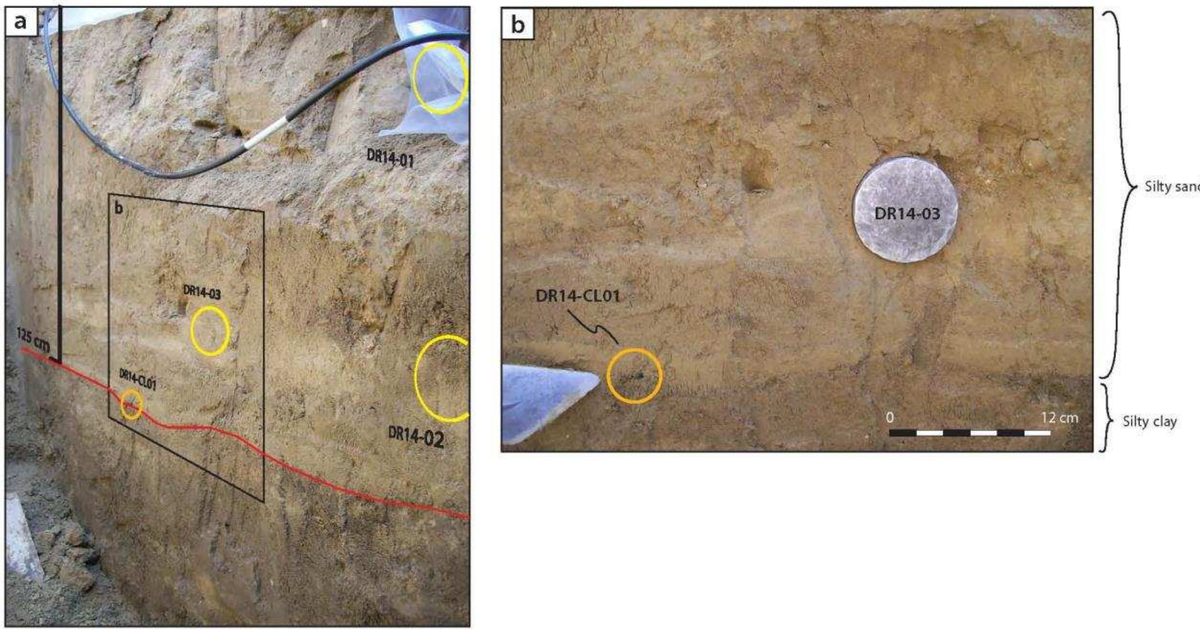

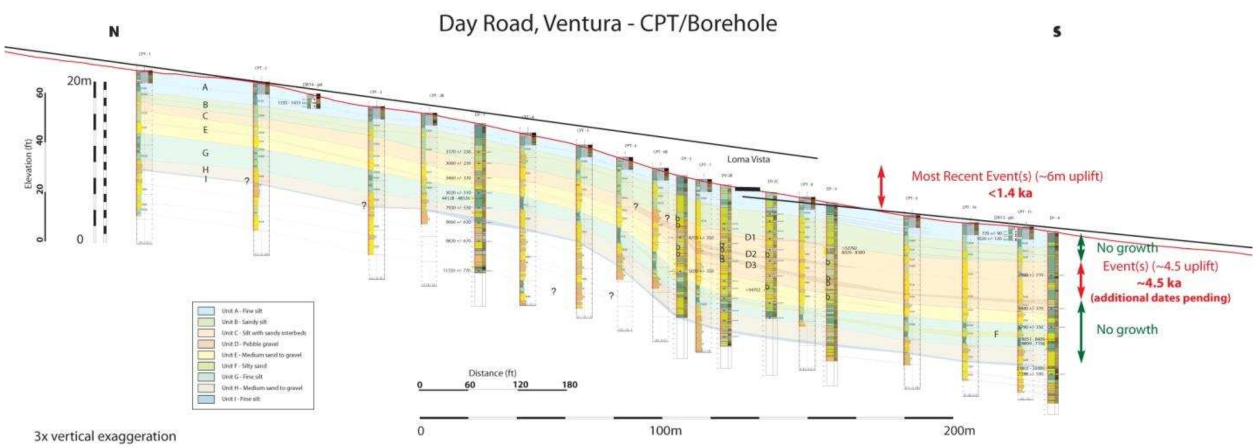

	Sample	Sample type	transect	borehole	actual depth, m	projected depth to borehole DY-4, m	Unit	Age (before AD 2013) 1 sigma uncertainty
	Dy-OSL-1/1	Luminescence	Day Road	Dy - 1	3.58	3.05	B	3170 ± 230
	Dy-OSL-1/2	Luminescence	Day Road	Dy - 1	4.95	4.26	C	3060 ± 230
	Dy-OSL-1/3	Luminescence	Day Road	Dy - 1	6.78	7.32	E	5460 ±330
	Dy-OSL-1/4	Luminescence	Day Road	Dy - 1	8.00	12.30	G	5020 ± 310
	Dy-OSL-1/5	Luminescence	Day Road	Dy - 1	10.44	14.78	H	7930 ± 530
	Dy-OSL-1/6	Luminescence	Day Road	Dy - 1	12.27	16.91	I	9060 ± 630
	Dy-OSL-1/7	Luminescence	Day Road	Dy - 1	14.40	?	Z	9820 ± 670
	Dy-OSL-1/8	Luminescence	Day Road	Dy - 1	18.21	?	Z	11720 ± 770
	Dy-OSL-2/1	Luminescence	Day Road	Dy - 2	7.70	9.29	C	4700 ± 350
	Dy-OSL-2/2	Luminescence	Day Road	Dy - 2	11.81	11.06	E	5070 ± 350
	Dy-OSL-4/1	Luminescence	Day Road	Dy - 4	5.41	5.41	C	2890 ± 210
	Dy-OSL-4/2	Luminescence	Day Road	Dy - 4	9.53	9.53	C	5480 ± 370
	Dy-OSL-4/3	Luminescence	Day Road	Dy - 4	11.81	11.81	G	4790 ± 350
	Dy-OSL-4/4	Luminescence	Day Road	Dy - 4	16.38	16.38	Z	7330 ± 500
Southern Pit	DR13-02	Luminescence	Day Road	DR13	1.08	0.76	A	770 ± 90
Southern Pit	DR13-04	Luminescence	Day Road	DR13	1.78	1.22	A	1020 ± 120
Northern Pit	DR14-02	Luminescence	Day Road	DR14	1.12	1.07	A	final dates pending as of the writing of this dissertation
Northern Pit	DR14-04	Luminescence	Day Road	DR14	1.58	1.37	A	final dates pending as of the writing of this dissertation
	DY-OSL-2B/3	Luminescence	Day Road	Dy-2B	7.24	5.79	C	final dates pending as of the writing of this dissertation
	DY-OSL-2B/4	Luminescence	Day Road	Dy-2B	9.37	9.29	C	final dates pending as of the writing of this dissertation
	DY-OSL-2B/5	Luminescence	Day Road	Dy-2B	11.81	10.36	E	final dates pending as of the writing of this dissertation
	DY-OSL-2B/8	Luminescence	Day Road	Dy-2B	15.47	14.33	G	final dates pending as of the writing of this dissertation
	DY-OSL-2B/10	Luminescence	Day Road	Dy-2B	18.67	17.56	Z	final dates pending as of the writing of this dissertation
	DY-OSL-2C/5	Luminescence	Day Road	Dy-2C	7.09	5.49	C	final dates pending as of the writing of this dissertation
	DY-OSL-2C/6	Luminescence	Day Road	Dy-2C	8.46	7.32	C	final dates pending as of the writing of this dissertation
	DY-OSL-2C/7	Luminescence	Day Road	Dy-2C	10.29	9.45	C	final dates pending as of the writing of this dissertation

	Sample	Sample type	transect	borehole	actual depth	projected depth to borehole DY-1, m	Unit	Cal. Yr. BP
	DY-C14	^{14}C	Day Road	DY-1	9.27	13.26	G	44128-48526
	DY-C12	^{14}C	Day Road	DY-3	5.94	4.42	C	>52792
	DY-C5	^{14}C	Day Road	DY-3	5.99	4.48	C	8029-8380
	DY-C1	^{14}C	Day Road	DY-4	13.46	13.46	G	8051-8409
	DY-C7	^{14}C	Day Road	DY-4	13.51	13.51	G	6899-7158
	DY-C3	^{14}C	Day Road	DY-4	16.69	16.69	I	23802-24446
Northern Pit	DY-14:CL-01	^{14}C	Day Road	DR14	1.26	1.07	A	1335-1415
	DY-2C:CL-1	^{14}C	Day Road	Dy-2C	12.06	10.51	E	>54702

Table 2. Uplift, along fault displacement, age limits, and estimated moment magnitude (Mw) for the two paleoearthquakes on the Ventura Fault from Day Road borehole and CPT results[a]

					M_w					
					Wells and Coppersmith (1994)				Biasi and Weldon (2006)	
					All-slip-type displacement		Thrust fault-only displacement			
			Slip (m)							
Event	Age (ka)	Uplift (m)	Min	Max	Min	Max	Min	Max	Min	Max
1	<1.4	6	7.32	8.49	7.64	7.69	6.75	6.76	7.91	7.98
2	3-5	4.5	5.49	6.36	7.54	7.59	6.74	6.74	7.76	7.84

[a]Based on the simplifying assumption that our measured displacements represent the average along fault slip in each earthquake
[b]Uplift is based on measured values from Day Road transect
[c]Slip is based on a fault dipping 50° ± 5° providing minimum and maximum slip values
[d]Biasi and Weldon (2006) incorporate the data of Wells and Coppersmith (1994)

Table 3. Earthquake magnitude estimates based on rupture area to magnitude regressions[a]

	M_w			
	Ventura fault	Ventura + Pitas Point	Ventura + Pitas Point + blind ramp	Ventura + Pitas Point + blind ramp + San Cayetano
Hanks and Bakun (2002; 2008)	6.07	6.63	7.09	7.45
Wells and Coppersmith (1994)	6.21	6.71	7.04	7.28

Fault segment	Area (km2)
Ventura	122
Pitas point	324.2
Blind Ramp	583.5
San Cayetano	884

[a]Fault area based on fault models produced by Hubbard et al. (in press)